Monitoring of Bond in FRP Retrofitted Concrete Structures

Ming Zhao, Yongtao Dong, Yang Zhao, Adam Tennant and Farhad Ansari

Journal of Intelligent Material Systems and Structures 2007; 18; 853 originally published online Apr 19, 2007;
DOI: 10.1177/1045389X06074571

Monitoring of Bond in FRP Retrofitted Concrete Structures

MING ZHAO,[1] YONGTAO DONG,[2] YANG ZHAO,[3] ADAM TENNANT[3] AND FARHAD ANSARI[3,*]

[1]*Department of Building Engineering, Tong Ji University, Shanghai, China*

[2]*Department of Civil and Environmental Engineering, University of Alaska Fairbanks P.O. Box 755900, Fairbanks, Alaska 99775-5900*

[3]*Civil and Materials Engineering, University of Illinois at Chicago 842 W. Taylor St. Chicago, Illinois 60607, USA*

ABSTRACT: Debonding failure of the concrete cover in reinforced concrete beams retrofitted with fiber reinforced polymer (FRP) composites is a brittle phenomenon which in most cases occurs in an abrupt manner. A complete understanding of bond requires information about the relationship between the local bond stress and slip. Bond-slip defines the constitutive relationship of the interface, and it provides means for computation of ultimate strength and distribution of the bond stress. For FRP composites interface slip is very small even at the ultimate stage prior to failure. For this reason, the study of local bond in the earlier studies did not include slip. This article presents a fiber optic based method for measurement of local slip at the interface between concrete and FRP as well as for prediction of bond failure in reinforced concrete members. Since bond failure in FRP retrofitted concrete is a brittle phenomenon, development of effective means to predict the failure prior to occurrence plays an important role in structural health monitoring of such structures. Therefore, the scope of the study includes two types of tests, namely pull out tests and beam flexure tests. In general, the measured interface slip between concrete substrate and FRP at ultimate load stage is $<60\,\mu m$. The fiber optic based system is capable of measuring the interface slip with a resolution of $1\,\mu m$. In flexure, the long gauge distributed sensors are able to predict the debonding and peeling of the FRP fabric from the concrete beam through deformation reversals. A numerical model based on finite element analysis of the beams is developed to verify the capabilities of the fiber optic sensor through computation of principal stresses at the interface.

Key Words: FRP, bond, slip, reinforced concrete, fiber optic sensors, distributed sensing, long gauge sensors, structural health monitoring (SHM).

INTRODUCTION

CIVIL structural applications of fiber reinforced polymer (FRP) composites include both new constructions as well as existing structures. FRP composites possess high strength to weight ratio and they can easily be employed for repair and flexural strengthening of concrete elements. In general, FRP is bonded externally to concrete by way of adhesives and transfer of the interfacial stresses to the concrete is governed through bond. The ultimate load carrying capacity of the retrofitted members is directly influenced by bond, and for this reason the subject has received much attention. In general, the study of bond and interfacial transfer of stresses has been investigated on two fronts, both at the local material level as well as at the elemental or structural level. At the local material level, study of bond has corresponded to pull out tests in a manner similar to the bond-slip tests traditionally performed in conjunction with steel rebars. Difficulties in conducting such tests with FRP are numerous including difficulties in measurement of slip due to the very small deformations of FRP prior to failure.

A complete understanding of bond requires information about the relationship between the local bond stress and slip. Bond-slip defines the constitutive relationship of the interface, and it will provide means for computation of ultimate strength, and distribution of the bond stress. Slip is defined as the relative displacement between the concrete and the reinforcement. In the case of reinforced concrete the chemical adhesion plays an insignificant role and the major portion of slip is associated with the transverse and longitudinal bond cracks. Such displacements are large enough and can be directly measured. For FRP composites, interface slip is very small even at the ultimate stage prior to failure.

*Author to whom correspondence should be addressed.
E-mail: fansari@uic.edu
Figures 2 and 7–15 appear in color online: http://jim.sagepub.com

1045-389X/07/08 0853–8 $10.00/0 DOI: 10.1177/1045389X06074571

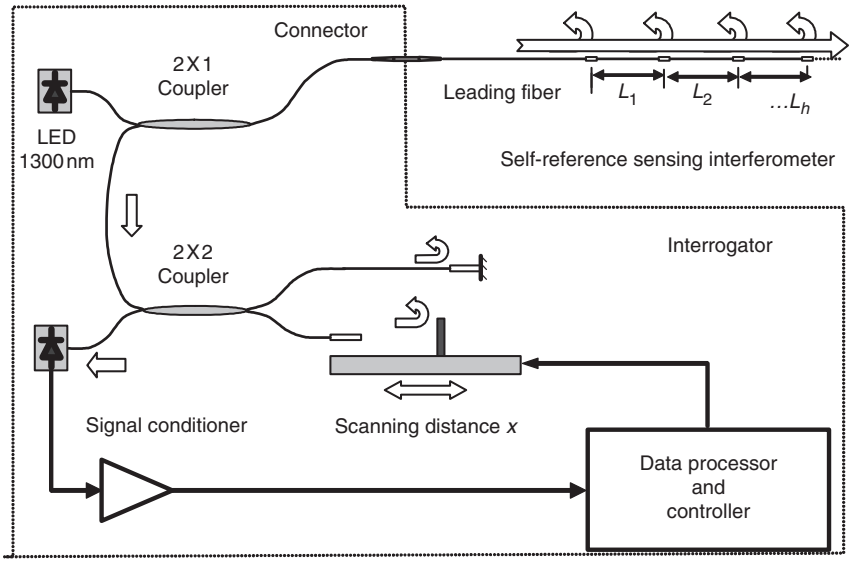

Figure 1. *Schematic representation of the distributed sensor and the interferometer assembly (Zhao and Ansari, 2001).*

In spite of these difficulties, a survey of the literature indicates that some investigators employed indirect methods for the measurement of slip in their work, including De Lorenzis and Nanni (2001) and Nakaba et al. (2001). Their research involved measurements and computations of slip indirectly through measurement of FRP strains. De Lorentzis and Nanni (2001) computed the slip based on direct integration of FRP strains assuming negligible displacements for concrete. Nakaba et al.'s (2001) specimens consisted of a tensile coupon with an embedded rod. Slip measurements were achieved by subtracting the FRP strains from the displacement of the test fixture that included the embedded steel rod, concrete, and the adhesive connected to the loading machine.

In view of the fact that the magnitude of slip at the interface between the concrete substrate and FRP is small, indirect measurements are subject to errors and a preferred approach is direct measurement of slip. Therefore, the first portion of the work presented here describes development of a testing fixture based on long-gauge optical fibers for direct determination of slip at the concrete–FRP interface. The second portion of the research presented in this article pertains to the use of long-gauge fiber optic sensors (FOSs) in the monitoring of bond and the detection of peeling failure in FRP retrofitted reinforced concrete beams. The term peeling is used here to distinguish the cover tension failure at the plane of the rebar from the debonding of the FRP at the adhesive layer from the concrete substrate. It is generally agreed that beams flexurally retrofitted with FRP fail either at the local level or in flexure through rupture of FRP or crushing of concrete (Buyukozturk and Hearing, 1998; Bonacci and Maalej, 2001). While the favorable mode of failure is flexural which is associated with large deflections, local failures do occur either by debonding at the concrete–FRP interface or in the plane of steel rebar due to the normal and shear stresses in concrete. In this latter mode of failure, it is believed that the existing reinforcing steel acts as a bond breaker in the horizontal plane, and the normal and shear stresses along the bonded FRP peel the concrete cover away from the rest of the member. The objective of this segment of the research was to assess the applicability of FOSs for the detection of the peeling failure prior to its occurrence. This portion of the research involved testing of FRP retrofitted reinforced concrete beams subjected to four-point bending. The experimental program is described next.

EXPERIMENTAL PROGRAM

The experimental program was designed to determine the bond-slip relationships as well as to assess the feasibility of using long gauge FOSs for monitoring the onset of bond failure and peeling in flexural members. Therefore, it was necessary to design two different types of specimens, test setups, and sensor configurations. The long gauge FOS system employed here operates based on the principle of white light interferometry (Yuan and Ansari, 1997). The main feature of the interferometric system employed in this study is the capability for serial multiplexing of the sensors.

The fiber optic distributed sensing system has been described elsewhere (Zhao and Ansari, 2001). A brief description is given here for completeness. The system consists of a sensing and an interrogation interferometer. The sensing interferometer is comprised of individual optical fiber segments of desired gauge lengths as shown in Figure 1. The individual fibers are mechanically connected and coated with a thin layer of

silver to achieve partial reflectivity. The interrogator, as shown in Figure 1 is a Michelson white light interferometer with a scanning translation stage, signal processing unit, and the control unit. The scanner automatically matches the displacements of the sensors and routes the sensed signals to the data acquisition system. The sensing interferometer is configured for automatic compensation of drift due to environmental effects, i.e., temperature. Experimental programs corresponding to local bond-slip tests are described first.

Bond-slip Tests

Determination of bond strength at the interface between FRP and concrete was accomplished by designing a specific test setup and sensor design to accommodate three different bond lengths of 80, 120, and 160 mm, respectively. The test setup consisted of bonding a 1 mm thick by 80 mm wide unidirectional carbon FRP (CFRP) fabric strip (SikaWrap 103C) to two sides of concrete blocks. The objective was to test the fabrics by pulling them away from the concrete blocks. The pull out load was applied by a closed-loop hydraulic actuator through a steel roller to avoid stress concentration and premature failure of the fabric. Strains along the FRP–concrete interface were measured by conventional strain gauges as well as fiber optic long gauge sensors (Figure 2). These sensors were adhered to FRP during the application of epoxy resin at the surface of the concrete substrate. The gauge length of the FOS was designed to cover the entire bond length of the FRP fabric.

The fixture shown in Figure 3 was designed for measurement of slip. It consisted of a metallic frame to establish reference with the concrete block, and an aluminum guide glued onto the protruding end of the FRP fabric. Slip was determined by measuring the relative movement of the guide with respect to the reference block. The relative displacement was measured by a long gauge optical fiber sensor whose ends were glued to the guide and the reference frame. The resolution of the interrogating interferometer for measurement of the displacements was 1 μm. Experimental results for local bond-slip measurements are given in the following section.

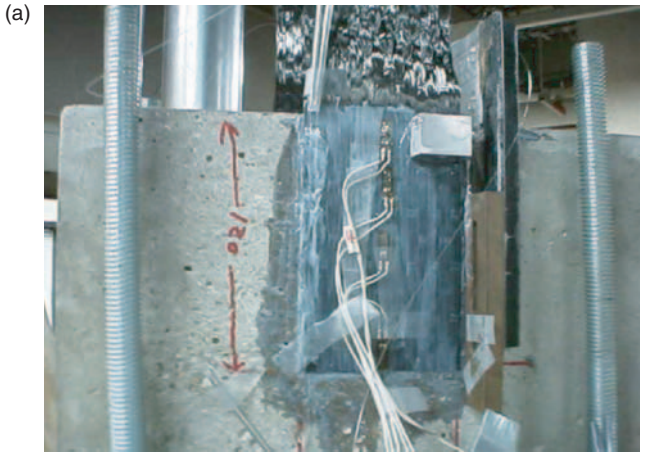

Figure 2. *Fiber optic sensor and strain gauges for measurement of FRP deformations.*

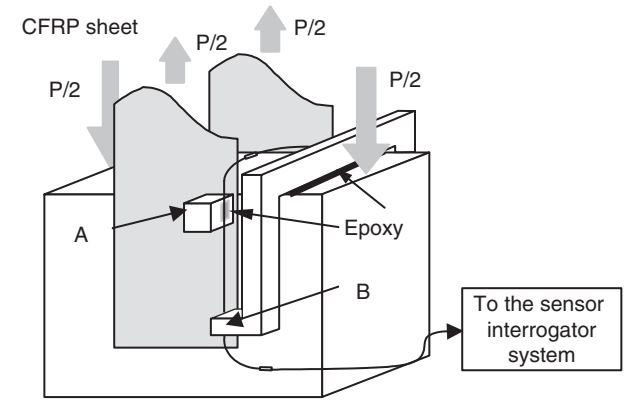

Figure 3. *Fiber optic interface slip measuring system.*

Monitoring of Bond Failure in Flexural Members

The experimental program to evaluate bond and peeling failure monitoring capabilities of the distributed FOS system involved testing of reinforced concrete beams under four-point bend loading configuration. Typical beam dimensions and reinforcement details are shown in Figure 4. Grades 60 and 40 steel rebars were used for longitudinal and shear reinforcements, respectively. The longitudinal reinforcements consisted of 16 mm and 10 mm diameter rebars with nominal yield strength of 410 MPa. The specimens were designed according to the ACI code. Three concrete cylinders were cast per beam for the determination of the compressive strength. The nominal compressive strength of the concrete employed for the construction of the beams was 38.2 MPa.

Preparation of beams for the application of CFRP involved sandblasting followed by airbrushing of

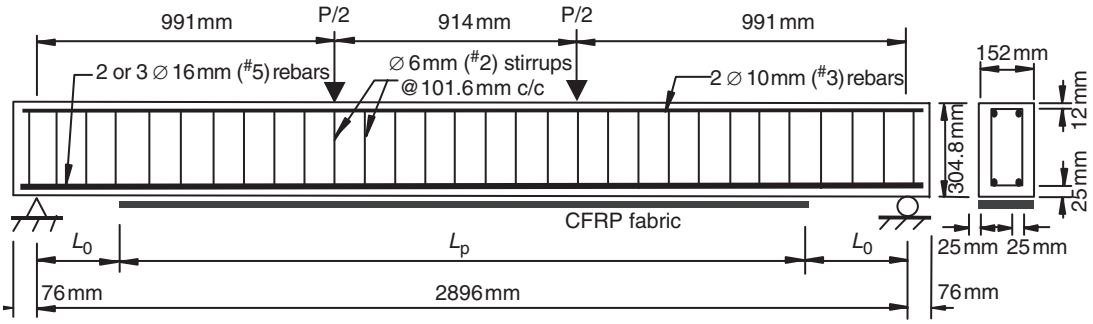

Figure 4. *Details of RC beam with bonded CFRP fabric subjected to four-point bending.*

Table 1. Beam specimen reinforcement details.

		CFRP system		
Beam no. (1)	Number of ∅ 16 mm steel rebars (2)	Thickness (mm) (3)	Length (m) (4)	Distance from CFRP end to support (mm) (5)
B0	2	NA	NA	NA
B1	2	2	2.134	381
B2	2	2	2.286	305
B3	2	2	2.744	76
B4	2	2	2.744	76
B5	2	4	2.134	381
B6	3	4	2.134	381

the tension face of the RC beams. A 1-mm thick unidirectional CFRP fabric (SikaWrap) with a two-component epoxy (SikaDur) was employed in the retrofit operations. The tensile strength, modulus of elasticity, and percent elongation of the CFRP system (fabric impregnated with epoxy) were 960 MPa, 73100 MPa, and 1.33%, respectively. The fabric was adhered to the specimens per manufacturer's instructions. The nominal thickness of the fabric/epoxy system for one layer was 2 mm. The fabric width was the same as the cross-sectional width of the RC beam and the lengths varied. Other specimen variables included the number of CFRP plies and the main internal steel reinforcement (Table 1). Beam B_0 was not retrofitted with FRP and served as the control specimen.

Beams were tested in a closed-loop testing system under displacement control. Each beam had a span of 2.9 m and loaded symmetrically about its centerline at two points 0.914 m apart (Figure 4). To simulate service load conditions, all the beams (except for B3) were preloaded until formation of several cracks in the region of constant moment and then they were repaired with CFRP fabric under the sustained load. Following the curing period of the FRP retrofit, the experiments involved monotonic loading of the beams until failure. Midspan deflections were measured by two linear variable differential transformers (LVDTs) on the two sides of the beam. Dial gauges were installed at the support points to monitor the vertical displacements of the support points. Electrical resistance strain gauges were employed for monitoring the midspan rebar strains.

Long gauge distributed optical fiber sensors were adhered to the surface of CFRP during impregnation of the composite with epoxy. These sensors were employed to monitor deformation and debonding of the CFRP fabric. The distributed sensor arrangement included four FOSs with gauge lengths of 152.4 mm each connected in series, and positioned from the curtailment of the CFRP sheet toward the centerline of the beam (Figure 5). By using four optical sensors in series, it was possible to monitor deformation over a length of 0.61 m along the span length each sensor monitoring the average strain over a length of 152.4 mm.

EXPERIMENTAL RESULTS AND ANALYSIS

Bond-slip Tests

The specimens were tested in a materials testing machine (MTS) under displacement control until failure. As shown in Figure 2, the specimens had two FRP–concrete interfaces on opposing sides of the specimen blocks. Both interfaces were instrumented with the strain gauges and the FOSs. Failure of bond would in general occur on one side of the block leaving the opposing interface intact. All the specimens failed through shearing of a concrete wedge at the protruding end of the FRP–concrete interface. Fiber optic sensor data correspond directly to the measured deformation along the entire interface length. Strain data from the strain gauges along the interface lengths were integrated to obtain the deformation.

Typical interface deformations measured by FOSs and strain gauges are compared in Figure 6. Data correspond to the failed as well as the intact interface sides of the concrete block. Examination of Figure 6 indicates lower interface stiffness for the failed side of the block when strain gauge data were used for the computation of the deformation. This difference is attributed to the fact that the single optical fiber averages the deformation across the entire interface length. However, the deformations

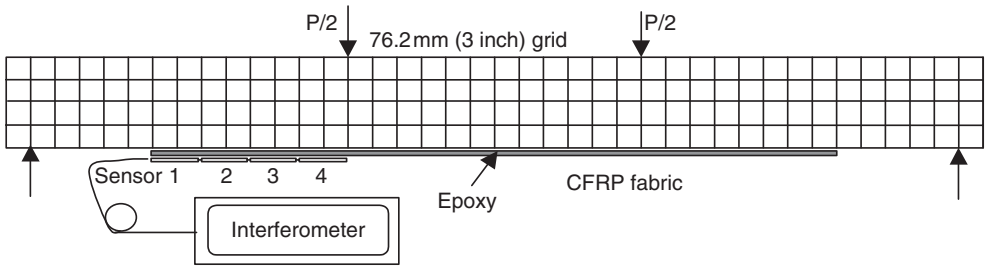

Figure 5. *Distributed fiber optic sensor for monitoring of bond.*

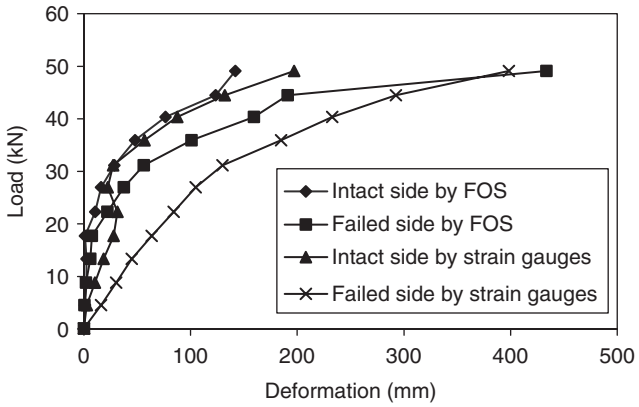

Figure 6. *Comparison of the fiber optic and strain gauge results.*

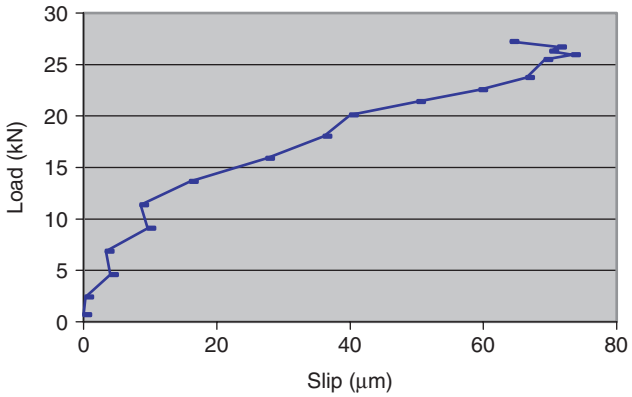

Figure 7. *Load vs slip relationship at the composite interface.*

computed through integration of strains from several gauges would include local strain spikes especially, since the failure was accompanied by cracking and shearing of the concrete block and redistribution of strains. Figure 7 corresponds to the typical values of end slip as measured by the setup shown in Figure 3. These measurements of end slips are very small even at the ultimate load stage. The fiber optic slip sensor was able to pick up cracking of the concrete wedge during the final stages of loading through the reversal of the end-slip trend.

Beam Tests

Table 2 provides information about the ultimate load and failure modes of the beams. The relationship between the load and the midspan deflections are shown in Figure 8. In comparison to the control beam, a strength increase ranging from 46 to 90% was observed for the retrofitted beams. Retrofitted beams also exhibited larger stiffnesses and reduced ductility when compared to the control beam. The control beam reached failure by crushing of the concrete long after the yielding of steel. All the other beams failed by peeling of the concrete cover (Figure 9) except for beam B3, which failed by debonding of the FRP from concrete along the adhesive layer (Figure 10). The measured rebar strains are shown in Figure 11. All the rebars yielded at the yield strain of 2500 με prior to reaching the ultimate load.

Experimental observations and measured fabric strains by FOSs provide insight as to the nature of the cover peeling failure. All the beams showed at first, a linear-elastic behavior followed by appearance of several flexural cracks in the midspan of the beam (Figure 12(a)). This stage of cracking continued up to about a fabric strain of 800 με (Figure 12(b)). During this first stage of cracking, the fabric end (Sensor 1) experienced rapid increase in strain, which is attributed to the larger concentration of stresses at the fabric end. No cracking was observed at the fabric end during the first stage of cracking (Figure 12(a)).

The second stage of cracking commenced at a fabric strain of about 800 με. At this point although no visible cracks were apparent until a strain of 1200 με, most of the strain was transferred from Sensors 1 and 2 to Sensors 3 and 4 away from the end. This is shown in Figure 12(b), where during a short period Sensors 1 and 2 recorded no increase in strain. The transverse shear crack at the fabric end was visible at about 1200 με. Although there were no visible indications of cover peeling cracks, the transfer of strain to Sensors 3 and 4 and an upward shift in the slope of strain in Sensor 1 indicated internal growth of the longitudinal peeling crack.

The third and final stage of cracking began at a fabric strain of 1500 με. At this point Sensor 1 went through a short unloading–loading–unloading period and continued unloading until an abrupt peeling failure. It is believed that the peeling crack had propagated in

Table 2. Beam test results.

Beam no. (1)	Load when FRP applied (kN) (2)	Ultimate load (kN) (3)	Midspan deflection (mm) (4)	Mode of failure (7)
B0	NA	104.44	70.17	Flexural
B1	28.18	157.28	31.86	Peeling
B2	23.29	164.76	24.31	Peeling
B3	0.00	183.79	34.17	Debonding
B4	25.83	198.46	34.70	Peeling
B5	24.07	183.26	20.40	Peeling
B6	26.23	181.42	20.97	Peeling

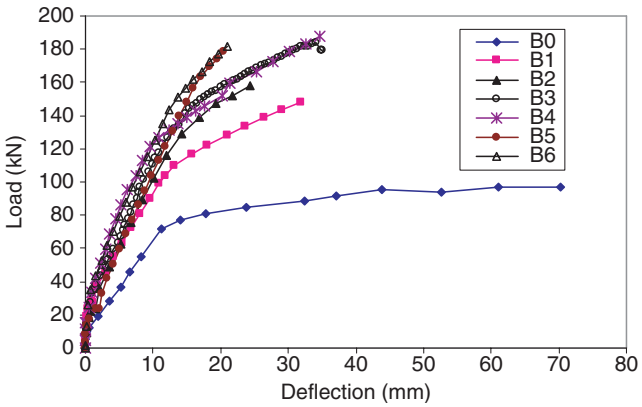

Figure 8. Load–deflection behavior of RC beams with externally bonded FRP.

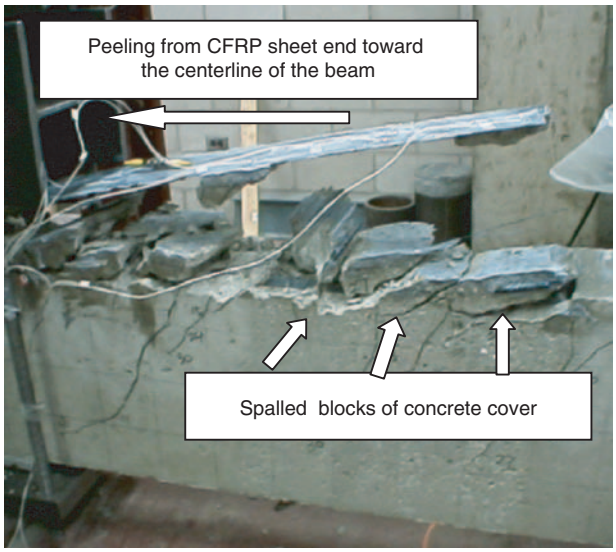

Figure 9. Peeling failure of concrete cover (Beam B2).

between the second set of transverse cracks since Sensor 2 had gone through a short dormant period without recording increase in strain.

NUMERICAL SIMULATION

Verification of sensor findings in terms of the cracking mechanism involved in the peeling was accomplished

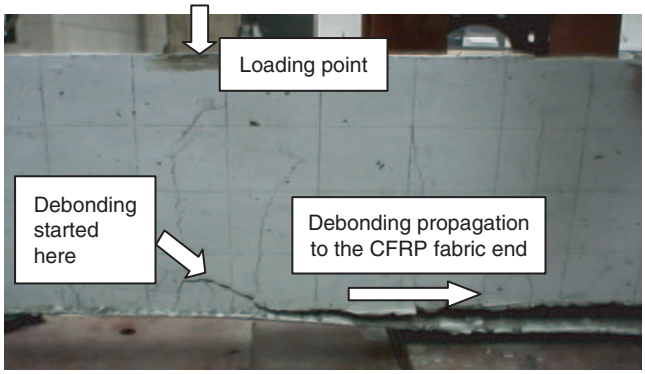

Figure 10. Debonding failure between FRP fabric and concrete (Beam B3).

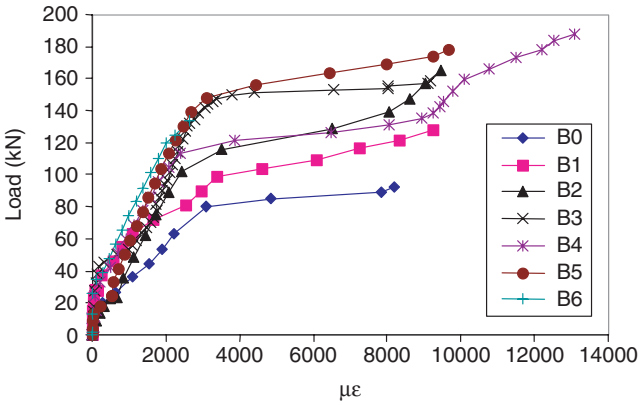

Figure 11. Rebar strains at the midspan of beams.

through numerical modeling. Finite element analysis was employed for computation of stresses and simulated the three-dimensional cracking pattern of the beams. Concrete was modeled by eight-node solid elements allowing nonlinear analysis with smeared crack/crush formulations. The concrete element was capable of cracking and crushing in three orthogonal directions. In order to investigate the stress distribution under the steel reinforcements, steel rebars were modeled by two-node spar elements linked to the concrete elements at nodal points. A bilinear elasto-plastic constitutive relationship was employed for the steel. The adhesive layer and CFRP fabrics were modeled using eight-node layered solid elements with linear elastic material properties.

To simulate the presence of FRP fabric, for the strengthened beam, the epoxy and FRP elements were kept activated throughout the analysis. In the repaired beams, the epoxy and FRP elements were deactivated until the attainment of the experimental pre-load values after which the fabric/epoxy elements were activated to simulate retrofit. Typical load–deflection characteristics repaired and strengthened beams are compared with the control beam in Figure 13. There were no major differences between the load–deflection responses of strengthened and repaired beams. Similar observations were found in RC beams strengthened with CFRP

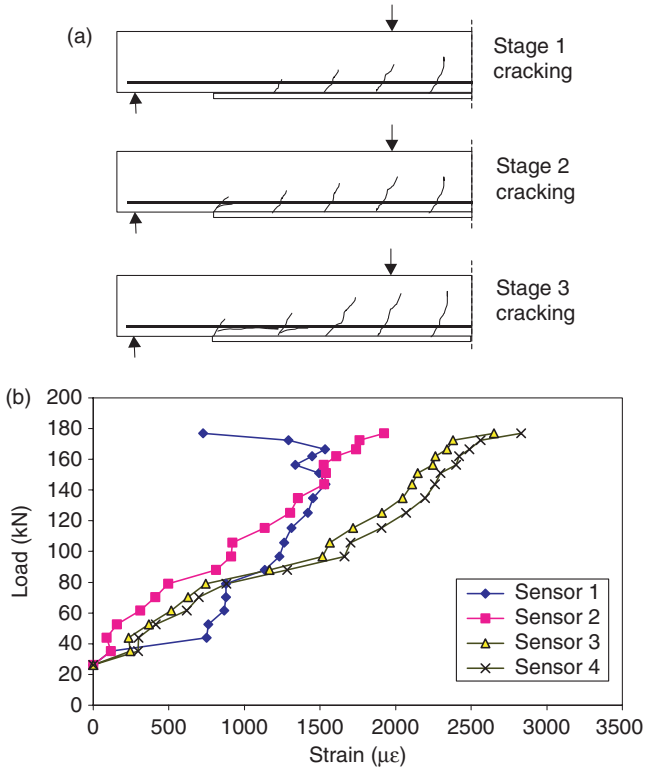

Figure 12. *Interrelationship between the strain distribution in CFRP and failure of the retrofitted beams. (a) Schematic depiction of cracking and failure process; (b) Strain distribution in the CFRP fabric measured by optical fiber sensors.*

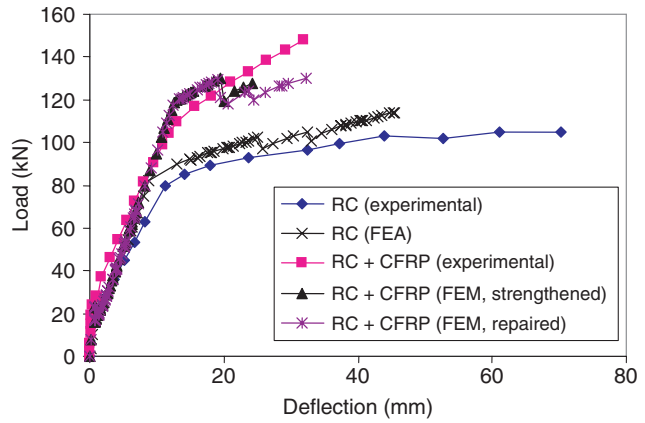

Figure 13. *Comparisons of numerical and experimental load–deflection relationships.*

sheets (Arduini and Nanni, 1997) and the bending tests of RC beams wrapped with carbon fabric (Gangrao and Vijay, 1998). Other researchers reported increase in ultimate loads after strengthening of severely damaged RC beams (Sharif et al., 1994).

The main objective of the numerical simulation was to assess the state of stress and their correspondence with the sensor predictions. Principal stress variations in the concrete cover along the steel reinforcement and the concrete–epoxy interface were computed and they are compared in Figure 14. The concrete under the rebar is

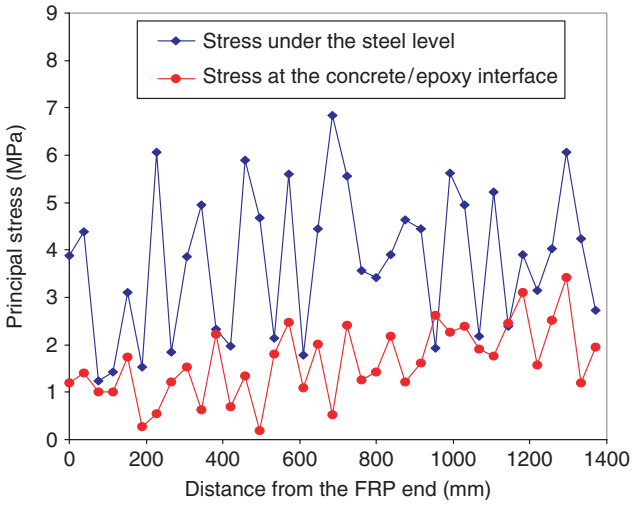

Figure 14. *Principal stress distribution under the rebar and at the concrete–epoxy interface.*

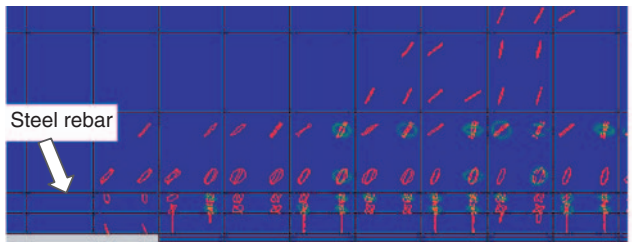

Figure 15. *Numerically simulated crack pattern in the retrofitted beam.*

subjected to higher stresses than those experienced in the adhesive layer within the FRP–concrete interface. Three-dimensional numerical simulation of cracking in the beam indicated formation of flexural cracks followed by shear flexure cracks and then by the commencement of cover cracks near the rebar (Figure 15). Upon further loading the inclined and horizontal cracks within the cover combine to peel off the concrete cover in between the transverse cracks. The circular and elliptical cracks in Figure 15 correspond to the three-dimensional inclination of crack surfaces. The crack surfaces underneath the rebar are parallel to the plane that encompasses the width and span of the beam.

CONCLUSIONS

Bond and peeling failure of FRP composites in reinforced concrete beams is a brittle phenomenon. Results from this study indicated that distributed fiber optic based systems provide effective means for structural health monitoring of FRP retrofitted elements. Furthermore, a method was developed for the measurement of slip at the interface between FRP and concrete substrate. In general, the measured interface slip between concrete substrate and FRP at ultimate load stage

was <60 μm. The fiber optic based system was capable of measuring the interface slip with a resolution of 1 μm. In flexure, the long gauge distributed sensors were able to predict the debonding and peeling of the FRP fabric from the concrete beam through deformation reversals. The applicability of the system is limited however, under increasing loads as the failure phenomenon is rather quick. Application of the sensor system developed here requires further experimentation for a complete understanding of the sensor signal based on member interface properties. A numerical model was developed to establish insight into the nature of stresses involved in such failure and verification of sensor results.

REFERENCES

Arduini, M. and Nanni, A. 1997. "Behavior of Precracked RC Beams Strengthened with Carbon FRP Sheets," *Journal of Composites for Construction*, 1(2):63–70.

Bonacci, J.F. and Maalej, M. 2001. "Behavioral Trends of RC Beams Strengthened with Externally Bonded FRP," *Journal of Composites for Construction*, 5(2):102–113.

Buyukozturk, O. and Hearing, B. 1998. "Crack Propagation in Concrete Composites Influenced by Interface Fracture Parameters," *International Journal of Solids and Structures*, 35(31–32):4055–4066.

De Lorenzis, L.M.B. and Nanni, A. 2001. "Bond of Fiber-reinforced Polymer Laminates to Concrete," *ACI Materials Journal*, 98(3):256–264.

Gangarao, H.V.S. and Vijay, P.V. 1998. "Bending Behavior of Concrete Beams Wrapped with Carbon Fabric," *Journal of Structural Engineering*, 124(1):3–10.

Nakaba, K., Kanakubo, T., Furuta, T. and Yushizawa, H. 2001. "Bond Behavior between Fiber-reinforced Polymer Laminates and Concrete," *ACI Structural Journal*, 98(3):359–367.

Sharif, A.M., Al-Sulaimani, G.J., Basunbul, I.A., Baluch, M.H. and Ghaleb, B.N. 1994. "Strengthening of Initially Loaded Reinforced Concrete Beams using FRP Plates," *ACI Structural Journal*, 91(2):160–168.

Yuan, L.B. and Ansari, F. 1997. "White-light Interferometric Fiber-optic Distributed Strain-sensing System," *Sensors and Actuators a-Physical*, 63(3):177–181.

Zhao, Y. and Ansari, F. 2001. "Quasi-distributed White Light Fiber Optic Strain Sensor," *Optics Communications*, 196(1–6):133–137.